EFFECTS OF A SIMULATED SLAG PHASES ON THE MIXING AND MASS TRANSFER RATES IN A 0.2-SCALE CREUSOT-LOIRE UDDEHOLM (CLU) CONVERTER MODEL

A. Chaendera & Rauf Hurman Eric
University of the Witwatersrand, South Africa

ABSTRACT

A gas jet was blown through submerged nozzles to stir the bath in the presence and absence of slag. Mixing and mass transfer rates were then studied. Kerosene (10% by volume) and water were used to simulate the slag and metal phases respectively in the cold model. The mixing time (T_{mix}) increased with bath height and decreased with an increase in the gas injection rate. Its value in the model vessel was related to gas flow rate (Q), bath weight (W), and bath height (H) by, $T_{mix} = 4.39Q^{-0.73}W^{0.24}H^{1.12}$. Inclusion of the slag phase increased Tmix by about 16% and the mass transfer parameter, $[(Re_{loc,r})^{0.25}(Re_t)^{0.32}]$, values by about 32%. Mass transfer rates were higher near the bath surface and in the gas-liquid plume region. They increased with gas flow rate but decreased with an increase in bath height. The relationship, $K\alpha Q^{0.08}$, showing derived mass transfer coefficient (K) dependence on the gas injection rate was established. The proportionality constant in the equation varied with gas flow rate and sample location. Turbulence characteristics inside the bath liquid were established to vary with location, vessel geometry and gas injection rate.

INTRODUCTION

Gas stirring plays a very important role in steelmaking processes. The gases purged into the converter bring about thorough mixing of the bath thus accelerating the physical and chemical reactions taking place in the vessel. Since inefficient stirring leads to a longer blowing period, the result is poor energy, time and vessel utilization. These factors impact negatively on the process economics as they increase the operating costs. Knowledge of the slag impact on mixing and mass transfer rates in the converter operation helps to accurately determine the necessary gas blowing rate for efficient stirring of the bath. Therefore, a thorough understanding of the slag phase influence on mass transport in the bath is vital for efficient operation of the CLU-converter. By combining the model and established empirical correlations it is possible to accurately predict the behaviour of the processes taking place in the industrial vessel.

Nyoka *et al.* [1] studied the process of mass transport in a Creusot-Loire Uddeholm converter using one-fifth scale water model experiments. Their investigations were conducted in the absence of a simulated slag phase. Their study would be referred to herein as, earlier work. The bath was stirred by air injection through five bottom-placed nozzles. The mixing conditions in the bath were evaluated in terms of the gas flow rate (Q) and bath weight (W) by $T_{mix} = 1.08Q^{-1.05}W^{0.35}$. The bath surface and the gas-liquid plume regions in the purged bath were identified as the zones exhibiting the highest mass transfer rates and turbulence effects. Lehner *et al.* (3) in their investigations immersed graphite rods into argon stirred melts of known composition for specified times. The dissolution pattern was found to be non-uniform, with the maximum dissolution rates occurring in the vicinity of the melt surface. The mass transport coefficients were largely independent of the bath depth away from the bath surface but showed a small increase towards the bath bottom. The results of several studies showed that the rate of mixing in metal processing operations depends on the rate of energy input or energy dissipation [2, 6, 7]. Investigations by J. K. Wright [4], showed that the dissolution rates of the rods outside the plume region were lower than the rates in the gas-liquid plume region at the same gas flow rate. The mass transfer rates were found to increase with gas injection rates.

Akdogan and Eric [5] established that the presence of a simulated slag layer caused an increase in the mixing time. That was explained in terms of the simulated slag layer tending to dissipate some of the input energy. In gas-stirred metallurgical vessels the turbulence caused by the gas-liquid plume rising through the bath facilitates the increase in mixing. Several researchers have come up with different mathematical relationships to explain the mass transport phenomenon in the reactors [6, 7]. Asai *et al.* [6], presented the results of earlier studies and their own cold model work in terms of the values of exponent n, in the relationship, $K \alpha Q^n$. Where n is the stirring factor of the gas flow rate (Q). Numerous values of n have been reported in various plant and pilot plant studies on the desulphurisation of steel as well as in many water model experiments.

Turbulence has been reported to play an important role in the mass transfer processes. J. Szekely *et al.* [8]. investigated mixing, the flow phenomena and mass transfer in argon stirred ladles. The mass transfer measurements obtained for the dissolution of carbon rods in argon stirred melts provided semi-direct confirmation of predictions made regarding the turbulence patterns within the system. The mass transfer rate was observed to increase with an increase in the stirring gas flow rate. Turbulence was directly related to the stirring gas flow rate in the converter. They also found that the local turbulence exhibited appreciable spatial variations. The vicinity of the plume recorded high levels of turbulence especially in the upper regions. Results from similar investigations by J.K. Wright [4] gave an approximately parallel-sided shape of the rods that were submerged in a purged molten bath with some necking at the surface. Plots of rod diameter against

immersion time showed that the rod diameter decreased linearly with immersion time thus, showing that the dissolution rates are constant for isothermal conditions. Therefore, in real systems the factors that affect the dissolution rates are:

- The method of introducing the additives
- The particle sizes of the additives
- The temperature of the bath
- The carbon content of the bath
- The gas stirring rates
- The chemical and the physical properties of the material being added.

EXPERIMENTAL MEASUREMENTS

The experimental set-up consisted of a clear cylindrical PVC tank that was one-fifth the size of the CLU-converter that was being simulated. The experimental work was divided into two parts, the establishment of the different zones in the bath and the bath mixing intensity measurements. Water and kerosene (10% by volume) were adopted to simulate the metal bath and the slag phase respectively in the model experiments conducted. Although a rigorous simulation of the actual CLU-converter was pursued, the top oxygen lance was not simulated in the investigation. The omission of the top lance was considered acceptable since it is not used continuously and for a long period of time during the actual blowing process in the commercial CLU-converter. Bath heights 0.56 m, 0.61 m, 0.67 m, 0.72 m and 0.78 m were investigated. Gas flow rates in the range between 0.010 m^3/s and 0.023 m^3/s were adopted for the investigations. The gas injection rates between the model and the real CLU-converter were related through the modified Froude number, 242 that was calculated for the industrial vessel. The bath height and gas flow rate were alternately varied in both sets of measurements.

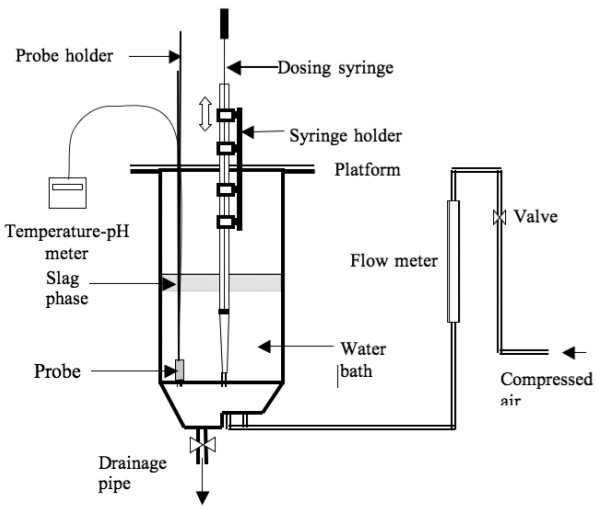

Figure 1: The general set-up of the apparatus used for mixing time measurements Chaendera *et al.* [9]

Bath Mixing Intensity Measurements

The experimental procedure used for this part of the investigation was the same as the one above. However, the location for the pH-temperature probe in the bath and the point for injecting the tracer solution were fixed. The experimental conditions that were adopted by Nyoka *et al.* [2] were also used for these investigations. The slag simulation procedure adopted in the current study provided the major difference. This was done to allow for a clear comparison of results obtained in the absence of slag and those in the presence of the simulated slag phase. The experimental runs were made at least 20 minutes long. An average of at least eight values obtained from different experimental runs was adopted as the mixing time under the investigated conditions. The experiments were carried out at different conditions of liquid bath height and gas flow rate. The mixing time was also calculated at 99.7% bath homogeneity, as opposed to the 95% bath homogeneity adopted by Nyoka *et al.* [2]. The effects of bath height, gas flow rate and the slag phase on the mixing behaviour of the bath were measured.

Mass Transfer Experiments

Solid-liquid mass transfer measurements were performed in a water-kerosene bath. The mass loss technique was employed to establish the mass transfer rates. The investigation involved measuring the mass losses on the benzoic acid specimens suspended in the gas purged bath for 15 minutes. Measuring the radii of the specimens that had undergone uneven dissolution during bath purging posed a challenge. Consequently, average radii were calculated from the weight losses recorded on the specimens. The experiments were divided into two parts. The first part was designed to establish results that could be used to explain the effect of bath height and gas flow rate on the mass transfer coefficients in the bath. Mass transfer coefficients were then calculated from the experimental data. The experiments were carried out at gas flow rates 0.010 m^3/s, 0.015 m^3/s and 0.023 m^3/s and water bath heights 0.4 m, 0.5 m and 0.65 m. The spatial positioning of the specimens in the experiments has been presented elsewhere Krishna Murty *et al.* [11].

RESULTS AND DISCUSSION

The results obtained were discussed in terms of the varying bath height and gas flow rate. The effect of these operating variables on mixing intensity and solid-liquid mass transfer was analyzed.

Generally, the mixing time was observed to decrease with increasing gas flow rate. Figure 2 below presents the effect of gas flow rate on the mixing time. This trend was explained in terms of the gas-liquid plume velocity changes that resulted from increasing the gas flow rate. At a constant bath height, as the gas flow rate increased the centre line plume velocity increased resulting in rapid recirculation of the bath that enhanced mixing. In earlier investigations [10, 11] it was noted that as the gas flow rate increased the plume cone angle increased thus increasing the plume radius at the surface and effectively increasing the plume volume in the bath. The effect of the enlarged high turbulence region was the enhancing of bath liquid circulation and mixing in the bath. The largest decrease in mixing time was observed at the highest bath height investigated, 0.78 m. The mixing time decreased by about 40% at this bath height but only by 31% at 0.56 m bath height. The observed changes in mixing time showed the possible depreciating influence of gas flow rate at higher levels of specific energy input.

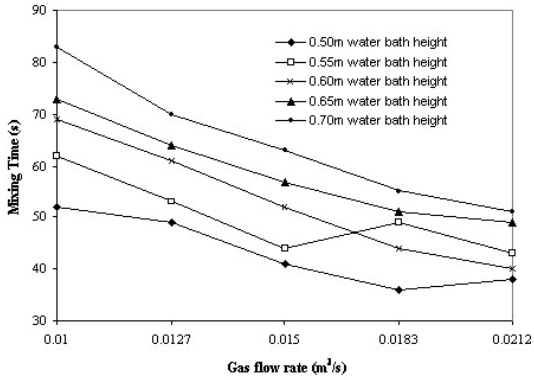

Figure 2: Effect of gas flow rate on the mixing time at different bath heights

Many researchers have observed the inconsistent behaviour of the mixing time shown in Figure 4 at 0.56 m and 0.61 m bath heights under different conditions [1, 4, 10, 12]. The seemingly consistent occurrence has been attributed to various reasons. The most convincing explanation was given by Mazumdar *et al.* [12]. They attributed the anomalies to zone shifting in the bath. In the current study, the probe was positioned in a generally 'slow moving zone' that was determined under specific conditions adopted in the preliminary experiments. Mixing rates in the various regions of the bath vary according to bath liquid activity or turbulence. Due to probable zone shifting, the probe was situated in a less active zone when the mixing time increased with an increase in gas flow rate. After this anomaly, it was observed that the mixing time at the 0.61 m bath height resumed the normal trend when it decreased after the gas flow rate was increased to 0.0212 m^3/s. It was therefore concluded that the new zone of activity was now determining the time taken for 99.7% bath homogeneity to be established. The existence of minimum mixing time values could have resulted from a probable swirling of the bath. Observations by Krishna Murty *et al.* [11], of the two-phase plume and flow conditions in the bath revealed that the plume swirled above a certain gas flow rate resulting in enhanced mixing rates in the bath. The minimum mixing times recorded in this study were therefore attributed to probable swirling of the plume that increased the rates of mixing in the bath.

The inconsistencies presented Figure 2 were observed at low bath heights and high stirring rates only. It was therefore argued that, the increases in mixing time values after a minimum was recorded were linked to the high specific energy input to the bath. Above a certain value of specific energy input, the level of tracer dispersion considered for the mixing time value to be determined could have been altered. Under conditions of very high stirring employed it was possible that, the partially affected zones in the bath were reached by the mixing power of the purging gases. The result was an increase in the volume of the bath liquid in the bulk flow regime and a consequent shifting of the equilibrium concentrations of acid in the two flow regimes at 99.7% bath homogeneity. Consequently, the mixing time increased against an increase in gas flow rate. As a result the mixing time values recorded tended to be longer than was expected, thus the abnormalities observed. It was therefore deduced that under these conditions the transfer of acid in the radial direction was lowered as the gas-liquid plume velocity in the axial direction increased. However at higher bath heights, it is apparent from the mostly positive gradients of the graphs in Figure 4 that the increased energy input to the bath reduced the mixing time. Better mixing in the bath was attributed to increased turbulence and bulk velocity of the agitated bath as the gas flow rate was increased.

Using the experimental results obtained, a correlation that could be used to relate the mixing time (*T*) to gas flow rate (*Q*) and bath weight (*W*) under the investigated conditions was established as,

$$T_{mix} = 2.87Q^{-0.73}W^{0.24} \quad (1)$$

The established correlation shows a greater influence of the gas flow rate on the mixing time than the weight of the load in the model CLU-converter. To get a clearer picture the effect of the bath height on mixing time was also investigated.

Effects of Bath Height on Mixing Intensity

For the gas flow rates investigated, the mixing time increased with an increase in the bath height as presented in Figure 3. The decrease in specific stirring energy input resulted in increased dead volumes at the bottom of the vessel and decreased bubble formation as the bath height increased thus, the reduction in mixing intensity observed. The bath height effect on the mixing time was greatest at the lowest gas flow rate as significant specific energy input changes were recorded here. An inconsistent variation of the mixing time and bath height was also observed.

As reported in literature, many researchers have observed the abnormal behaviour of the mixing time in gas stirred baths under different conditions [1, 6]. The occurrence of peaks in Figure 3 at gas flow rates 0.0183 m^3/s and 0.0212 m^3/s was attributed to zone shifting in the bath. A peak was observed when a quieter zone occupied the point where the probe was located. Assuming this was the case then, the mixing times recorded were bound to be the opposite of what was expected since mixing rates in the various regions of the bath vary according to activity or turbulence.

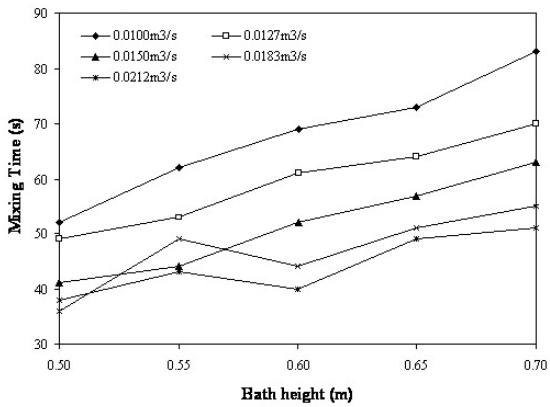

Figure 3: Effect of bath height on the mixing time

The mixing pattern at bath heights above 0.61 m could be explained in terms of the columnar effect becoming pronounced with an increase in bath height. Castillejos and Brimacombe and Asai *et al.* [14, 6] discussed that at high ratios of bath height to diameter of the vessel, dead volumes that formed near the bottom of the vessel had the effect of increasing mixing time. Murthy *et al.* [11] explained this phenomenon by means of a multiple circulation model, in which the bath consists of several circulation cells in the axial direction that make mixing by bulk flow ineffective. The formation of the circulation cells

in the bath inhibits the thorough mixing of the bath solution. Thus, longer periods of mixing are observed under conditions of increased bath load as more circulation cells are formed. When the formation of circulation cells in the bath occurs at lower bath heights, the mixing time that is recorded tends to be longer than the expected value. The multiple circulation cells model could be used to explain the large mixing time values recorded at the 0.61 m bath height and gas flow rates of 0.0183 m^3/s and 0.0212 m^3/s. The deviation from the 'normal' depends on the extent of circulation cells formation. Using this model, the formation of circulation cells in the bath was therefore more pronounced at the gas flow rate of 0.0183 m^3/s than at 0.0212 m^3/s.

The bath height in the vessel that had a diameter of 0.5 m was observed to have the largest effect on the mixing time. Using the experimental results obtained, a correlation that could be used to relate the mixing time (T) to gas flow rate (Q), bath weight (W) and bath height (H) was established as,

$$T_{mix} = 4.39Q^{-0.73}W^{0.24}H^{1.12} \quad (2)$$

The mixing time values estimated from this correlation had an average deviation of ±3% from the experimentally determined values. Figure 4 below presents a comparison of the mixing time estimates obtained using the two correlations established.

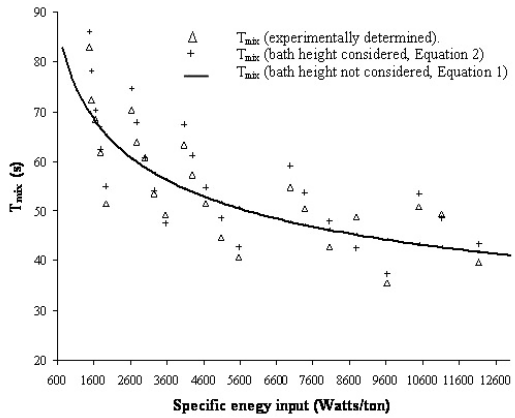

Figure 4: A comparison of the deviations of the estimates from the experimentally determined mixing time values

The crosses in Figure 4 above represent the sample points estimated by Equation 2 and the solid line by Equation 1. The sample points that were determined taking the bath height into consideration, i.e., +, are closer to the experimentally determined values represented by the triangles, Δ. These two corresponding values can be identified in Figure 4 by checking points falling on the same specific energy input line. The solid line in Figure 4 was plotted from the points calculated from the relationship that did not take the contribution of the bath height into account.

Effect of the Simulated Slag Phase on Mixing Time

The effect of slag was established by comparing the results of the current study to those obtained by Nyoka *et al.* [1]. Longer mixing time results were recorded because of the increased load coming from the incorporated slag phase. The influence of tracer

partitioning between the two liquids constituting the bath also prolonged the mixing time further. Since the incorporated slag phase constituted only 10% of the bath, it was argued that the reduced mass transfer rates of the tracer in the bath liquid had a huge influence.

Investigations by Akdogan and Eric *et al.* [10] centred on measuring the rate of transfer of a tracer from the water phase to the kerosene phase. They reported that the time taken for the tracer to distribute into equilibrium partitioning ratios was a variable of gas flow rate, bath height and nozzles configuration. As a result of the density differences of the kerosene and water, the purged liquid at the bottom of the bath where dosing was effected had a greater proportion of water than kerosene. The consequence of that was the prolonging of the mixing time as an equilibrium portion of tracer had to be transferred to the larger part of the slag phase in the dynamic fluid system.

It was possible to determine the effect of the slag phase on mixing intensity by considering the mixing time correlations obtained in the presence and absence of the simulated phase. The mixing time values predicted using the established correlations were compared on the basis of their variations with specific energy input to the water bath. Figure 5 presents a comparison of predicted mixing time values when the baths were at the same water bath height but had different weights because of the slag included in the other case. It is apparent from the graphs in Figure 5 that the mixing time increased with the inclusion of the slag phase. It took a longer period for the same energy input to cause the same level of mixing on an increased bath volume. The slag phase dissipated some of the input energy to the bath. Thus, higher mixing time values were recorded. The effect of the slag phase increased with the specific stirring energy density. The exponential relationship between the stirring power and the gas injection rate results in a marginal decrease in gas flow rate reflecting as a huge reduction in the stirring power in the converter. Slag inclusion reduced the mean gas velocity in the bath. Thus, an increased change in mixing time value was observed when the specific energy input increased. These observations indicated the significance of kinetic energy at high specific stirring energy density. Under conditions of high bath weight, the kinetic energy factor of input energy has relatively less effect on mass transfer rates that are mainly controlled by buoyancy energy. Other factors therefore become more significant in influencing the mixing behaviour of the bath.

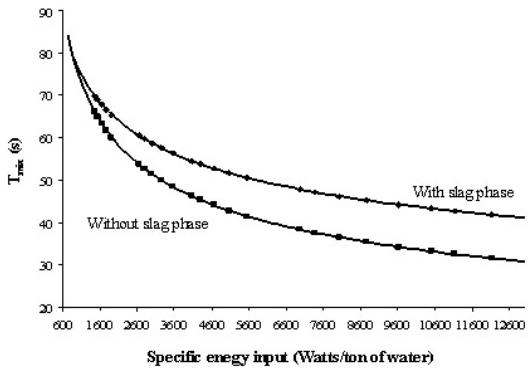

Figure 5: Effect of the slag phase inclusion on the mixing time values predicted for model converter operation

At lower stirring rates, the bath took long periods to homogenize. The extended period observed during bath homogenization allowed the tracer enough time to partition itself, in equilibrium amounts, between the two phases making up the bath liquid. This occurred in almost the same time as it would have in a single phase. This was the reason why the

mixing time change with the inclusion of the slag phase was small at lower specific energy input than at high specific energy input. Under the later conditions, bath homogeneity was quickly achieved in a single phase bath. Thus, the inclusion of a second phase tended to prolong the mixing time more as the tracer distributed itself in a bath that was not homogenous. The different kerosene-water proportions at the bottom and surface was responsible for the inhomogeneity of the bath liquid. In the absence of stirring or at very low stirring rates, mixing of the tracer is mainly controlled by convection forces that are less affected by a second phase inclusion. Therefore, the mixing time values were predicted to converge or to be very close at some point as the specific energy input was lowered. An average change in mixing time of 16% was observed for the conditions investigated.

The effect of slag inclusion was clearly shown by graphical comparisons of the results in Figure 5 above. The graphs in Figure 6 to Figure 15 below present the effect of the simulated slag phase under the different conditions investigated.

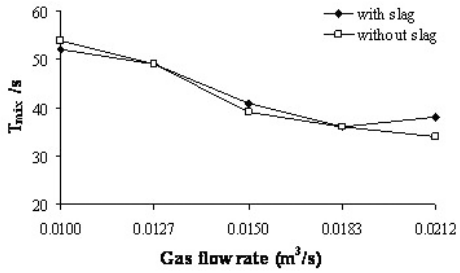

Figure 6: Mixing time variation with gas flow rate at a water bath height of 0.50 m

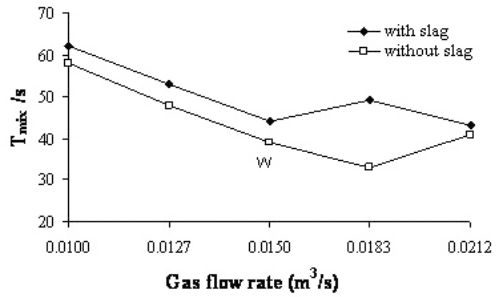

Figure 7: Mixing time variation with gas flow rate at a water bath height of 0.55 m

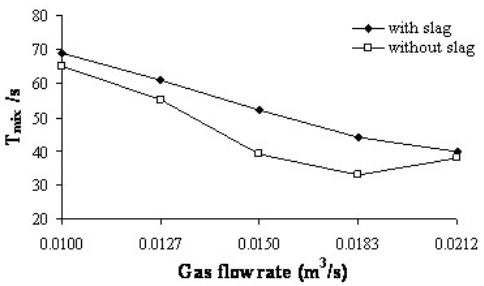

Figure 8: Mixing time variation with gas flow rate at a water bath height of 0.60 m

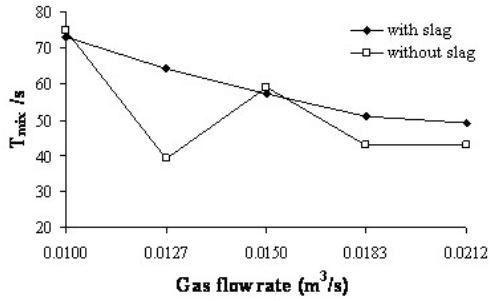

Figure 9: Mixing time variation with gas flow rate at a water bath height of 0.65 m

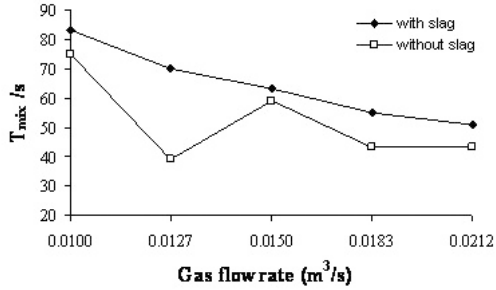

Figure 10: Mixing time variation with gas flow rate at a water bath height of 0.70 m

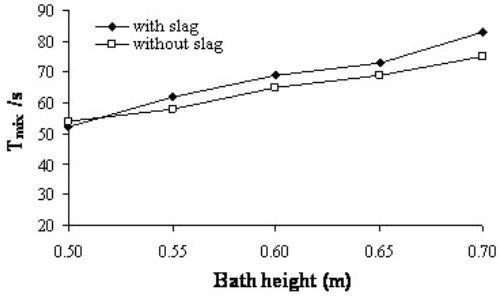

Figure 11: Mixing time variation with bath height at a gas flow rate of 0.010 m^3/s

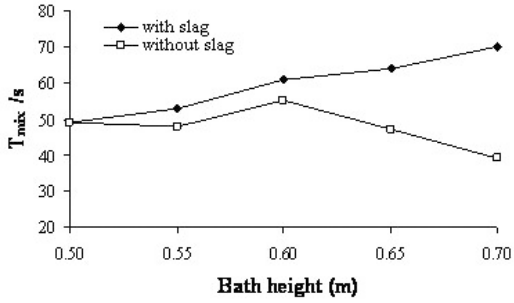

Figure 12: Mixing time variation with bath height at a gas flow rate of 0.0127 m^3/s

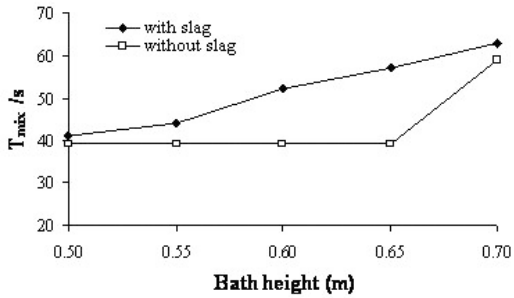

Figure 13: Mixing time variation with bath height at a gas flow rate of 0.0150 m^3/s

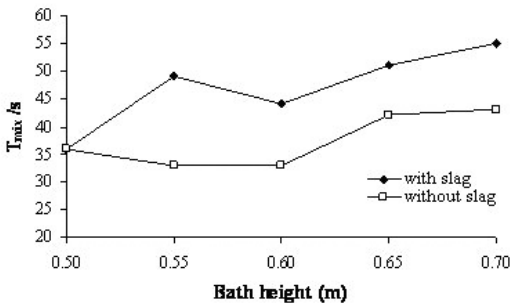

Figure 14: Mixing time variation with bath height at a gas flow rate of 0.0183 m^3/s

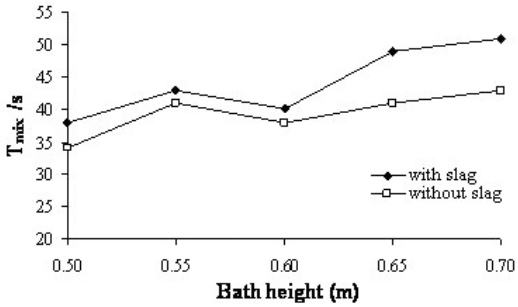

Figure 15: Mixing time variation with bath height at a gas flow rate of 0.0212 m^3/s

The graphical presentations gave substance to the observations that were based on the presentation given in Figure 5. It is apparent that the inclusion of a second phase had the effect of increasing the mixing time. The difference in mixing time values was lesser at lower bath heights where the specific input rates were lower and vice versa. The effect of the simulated slag phase was further emphasized by comparing the mixing time values that were obtained in the current study both in the presence and absence of the simulated slag phase. An average value of the percentage change in mixing time was calculated from these results to be, 17%. The value compared quite well with the 16.3% value obtained from Figure 7 presentation. The close similarity of these percentage changes in T_{mix} values as presented is important. The similarity exhibited gave substance to the comparisons of the mathematical relationships, Figure 5, and the assumption made on the similarities of levels of homogeneity considered in the two cases. It was therefore concluded that the analysis presented gave a true picture of the influence of the slag phase on mixing in the model bath. The comparison of the two investigations was therefore considered successful.

Differences in the Way the Collected Data was analysed

For a meaningful comparison of the mixing time values obtained in the two cases to be made, the degree of mixing considered had to be the same or almost so. The two sets of work were successfully compared by carefully taking into consideration the difference in the way the collected data was analyzed. Whilst there seem to be a big difference in the homogeneity levels considered, the matter-of-fact is that, these two cases considered mixing time at almost the same level of tracer distribution.

In the current study homogeneity of the bath was defined at 99.7% whilst the earlier work(2) defined it at 95%. The seemingly pronounced difference in the levels of homogeneity adopted in the two situations emanated from the difference in the definitions of homogeneity of the bath solution that were used. Whilst in the earlier work the effect of temperature changes on the pH of the bath was not taken into consideration, the values of mixing time obtained in the current study took into account the effect of these changes.

Observations from the performed experiments did not agree with the assertion made in the earlier work that there exist stable pH values [2]. The pH values recording on the meter were never stable for long periods of time during the 20 minutes long experiments conducted. This has been explained to be a result of a drop in bath temperature caused by the cold compressed air that was used for purging the bath. The relationship between temperature and pH is well represented by the Nernst's equation. As a result, temperature

compensation of the bath pH was performed the current study. That had the effect of raising the pH level of the solution when a defined homogeneity was supposedly reached. As a result, approximately the same pH value that was defined to describe homogeneity at 95% was used to check for the mixing time at 99.7% homogeneity after temperature compensation. On the basis of this argument, it was reasonably assumed that the level of homogeneity considered in both cases was almost the same. In other words, the bath homogeneity level defined as 95% in the earlier work was approximately defined as 99.7% in the current study.

Effect of Gas Flow Rate and Bath Height

The solid-liquid mass transfer rates in different regions of the bath were represented by calculated mass transfer coefficients. Figure 16 presents an example of the effect of increasing gas flow rate on mass transfer coefficients in the bath.

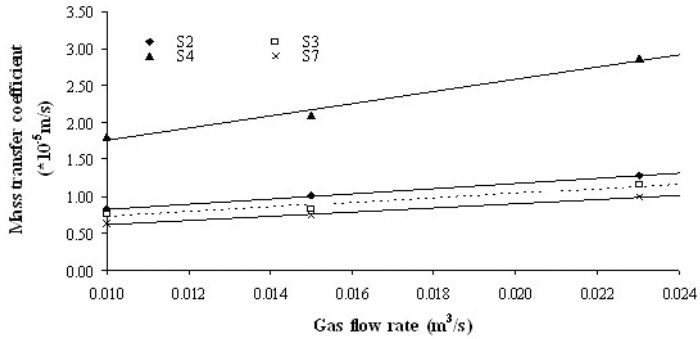

Figure 16: Effect of gas flow rate on mass transfer coefficient at 0.44m bath height

The increased stirring power imparted by the purging gases was responsible for increasing the energy needed to erode and support the dissolution of the benzoic acid specimens. At a constant bath height, as the gas flow rate increased the centre line plume velocity increased resulting in rapid recirculation of the bath that enhanced mixing. The plume cone angle was observed to increase with gas flow rate thus effectively increasing the plume volume in the bath. The effect of the enlarged high turbulence region was the enhancement of circulation, mixing and solid-liquid mass transfer in the bath. Significant mass transfer rates were observed near the bath surface. The weight of the much reduced overlying liquid near the bath surface promoted the multiplication of the rising air bubbles in the buoyancy energy dominated region. Under these conditions more stable gas bubbles were formed, thereby promoting turbulence and mass transfer. The wave action, splashing and eddies caused by the gases leaving the bath at high velocity markedly enhanced the dissolution rates of benzoic acid specimens in the region.

Mass transfer coefficients were almost constant inside the bath but increased slightly at the bottom. Samples S2 and S7 were located inside the bath but outside the highly turbulent gas-liquid plume. Sample S3 was in the, eye, transition region between the turbulent gas plume region that was originating from the nozzles and the recirculation liquid from the bath surface. The kinetic energy of the bath liquid and bubble formation were lower in these zones. Mass transfer rates in all the low turbulent regions were dependent on the generally low energy levels of the bath liquid and the dissolved acid levels in those localities. The presentation in Figure 16 shows that there was almost uniform change in

the mean mass transfer rates as the gas flow rate increased. Comparable gradients of the plots indicated an almost constant effect of increased stirring power on the mass transfer coefficients inside the bath. The gradient of the graph observed at Sample S4 is slightly steeper indicating the influence of more turbulence that existed in the region close to the bath surface as the gas flow rate was increased. The results obtained were consistent with the observations made in earlier investigations. The mass transfer coefficient was highest close to the bath surface, lower and almost uniform inside the bath before increasing slightly at the bottom of the vessel. The spatial positioning of the benzoic acid specimens in the three regions influenced the observed mass transfer characteristics. The geometry of the bath also modified the mass transfer characteristics of the bath in certain locations, especially close to the step at bottom.

Increasing bath height reduced the mass transfer properties in the model converter. Figure 17 below presents the effect of bath height on the mass transfer coefficient. The negative gradients of the graphs resulted from reductions in specific bath energy as the bath load was increased at a constant gas flow rate. The change in mass transfer coefficients was gradual for most locations at 0.010 m^3/s gas flow rate. However, the gradients of the graphs became steeper as the gas flow rate increased. The sensitivity of mass transfer coefficients at higher gas flow rates was attributed to a much larger specific energy input drop as the bath height was increased. As the load increased, input energy dissipation also increased hence the reduction in the specific input energy to the bath. The exponential relationship that exists between mass transfer and the gas injection rate was also responsible for greater sensitivity of the mass transfer coefficients at higher gas flow rates.

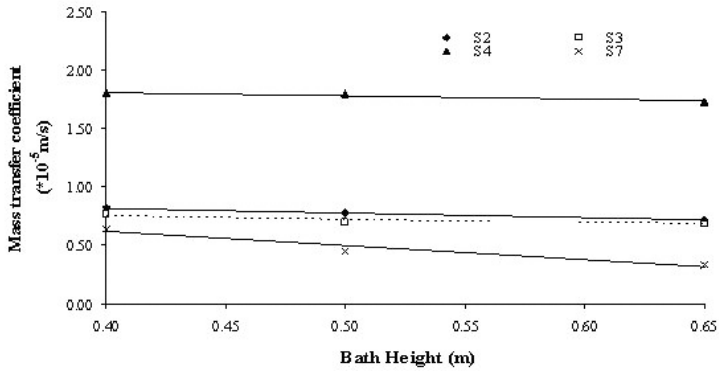

Figure 17: Effect of bath height on mass transfer coefficient at 0.01 m^3/s gas flow rate

Mass Transfer Coefficient Variation with Gas Injection Rates

Turbulence in gas-stirred metallurgical vessels was established by Akdogan and Eric [5] to be a result of the gas-liquid plume rising through the bath. An increase in mass transfer rates was attributed to increased turbulence in the bath. Several researchers have come up with different mathematical relationships to explain the mass transport phenomenon in the reactors [6, 7]. Asai *et al.* [6], presented the results of earlier studies and their own cold model work in terms of the values of exponent n, in the relationship,

$$K \alpha Q^n \tag{3}$$

Where n is the stirring factor of the gas flow rate (Q). Numerous values of n have been

reported in various plant and pilot plant studies on the desulphurisation of steel as well as in many water model experiments. The variation of the mass transfer coefficient was related to the gas flow rate using linear regression analysis to establish the coefficients of Equation 4 below,

$$K = mQ^{n} \tag{4}$$

The value of the coefficient m, was not constant as it is a variable of many quantities. Its value depended on fluid properties, vessel geometry, bath height, sample location and the gas stirring rate. For this reason the relationship expressing the variation of the mass transfer coefficient in various positions of the bath and operational conditions took the form Equation 7. Since the standard deviation of the values of n was low, an average of all the calculated values, n=0.08, was adopted to give the relationship in Equation 5 below,

$$K \alpha Q^{0.08} \tag{5}$$

The value of the factor n has been reported in literature to vary between approximately 0.25 and 2.10 [6]. However, the value established in this study was considered valid since it was established under more intense stirring conditions than those reported. At very high gas blowing conditions used in the CLU-converter, the effect of gas flow rate on mass transport becomes less pronounced. Thus, the low value of the stirring factor, 0.08, of the gas flow rate obtained. The observation made is supported by the work done by J.M. Chou *et al.* [15] and J.K. Wright [4]. In their studies of mass transport, they established that the mass transfer rate increased with gas flow rate. The mass transfer coefficients initially increased strongly with the gas flow rate, but this effect diminished with further increases and lower stirring factors were observed at higher gas flow rates. The dissolution rates were observed to be significantly higher in the plume region than in the other parts of the bath.

In separate investigations on mass transfer between two phases, J.M. Chou *et al.* [15] established that the mass transfer rate increased with gas flow rate. They attributed this to better mixing of oil and water in the cold model. As the gas flow rate approached 0.000 67 m^3/s the improvement in the mass transfer rate with gas flow rate became less obvious. In the same studies, the value of n was established as 0.39 regardless of sampling location when the gas flow rate was less than the critical gas flow rate, 0.000 67 m^3/s. However, this value was 0.032 when the gas flow rates were increased above the critical level. The stirring factor, 0.08, established was therefore assumed valid as the gas flow rates used were much higher than the reported critical value even if the model used was smaller.

Effect of the Slag Phase on Mass Transport

A comparison of mapping results obtained in the absence and presence of the simulated slag phase was done to establish the effect of the simulated slag phase. Comparisons of the respective mass transfer coefficients obtained in the model experiments are presented in bar charts below. The results of the experiments showed that the mass transfer values were lowered by the inclusion of the slag phase. This was attributed to an increased bath load reducing the specific stirring energy under the given conditions. Although to a lesser extent, the change in the dissolving capacity of the bath solution as a result of increased viscosity reduced samples' dissolution when the slag phase was included. The decrease in the mass transfer coefficients with slag inclusion were not constant but averaged 19.3% for all the gas flow rates investigated in the bottom region. The decreases were about 26%,

14% and18% for the gas flow rates 0.010 m^3/s, 0.015 m^3/s and 0.023 m^3/s respectively. The changes in mass transfer coefficients were highest at low gas flow rates. This was explained by the fact that, when stirring energy is low any opposing energies or factors result in a large change in mass transfer coefficients. The effect was minimised as the gas flow rate increased, resulting in increased stirring energies, whereas the retarding factors remained almost unchanged.

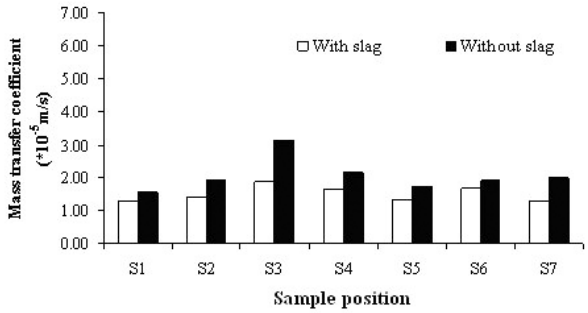

Figure 18: Comparison of mass transfer coefficient values at a gas flow rate of 0.010 m^3/s in the bottom region

As presented in Figures 8 above, the mass transfer coefficient in the bottom region were higher in experiments performed in the absence of the slag phase. For both investigations considered, mass transfer coefficients were generally higher in the regions close to the nozzles where Samples S3, S4 and S5 were located. The step at the bottom of the model converter was responsible for increased turbulence in its vicinity thus, the higher mass transfer rates observed on Sample S3. Mass transfer rates in the bottom region increased with purging gas flow rate. An increase in gas flow rate resulted in increased stirring power in the bath hence, more erosion and/or dissolution of the suspended samples. However, the mass transfer rates in this region were generally low because the samples were placed at the end of the bath liquid re-circulating loop. The liquid in this region had lost much of its kinetic energy thus, the eroding power. Turbulence was therefore limited as gas bubbles were only confined to regions in the vicinity of the nozzles.

The presentation in Figure 9 below is an example of comparisons of the mass transfer coefficients near the cone region. The samples were located slightly above the nozzles, where the cylindrical section of the vessel started. A greater influence of the gas-liquid plume in this region became apparent. As a result of the close vicinity of the nozzles to the region, Samples S4 and S5 that were located inside the high turbulent gas-liquid plume experienced much increased mass transfer rates. Compared to the values in the bottom region, lower mass transfer coefficients were recorded at Location S3 for all gas flow rates investigated. The lowering of mass transfer coefficients showed the decreasing influence of the step as the samples moved further away.

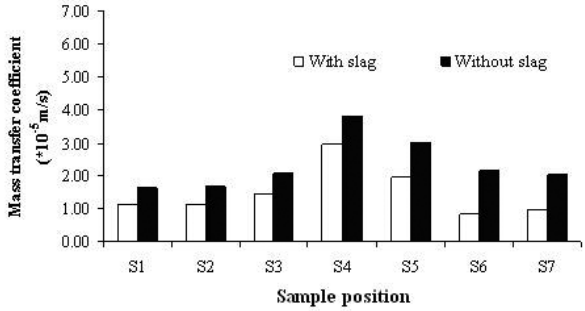

Figure 19: Comparison of mass transfer coefficient values at a gas flow rate of 0.010 m^3/s near the cone region

Generally the mass transfer rates were higher in the bottom region than near the cone region for positions that did not fall inside the plume. The mass transfer coefficients decreased near the cone region except for Locations S4 and S5. This was attributed to the fact that these samples were not located inside the plume region thus, the marginal mass transfer rates observed. The mass transfer rates followed the turbulence patterns that were exhibited in the bath. Two distinct regions were observed in the near cone region. There was a region that fell inside the plume and another one that was extending from the vessel walls to the interface, eye of the bath liquid, between the re-circulating liquid and the plume region. Existence of dead volumes in the latter region was quite probable. Under conditions of low gas purging, slow moving kerosene droplets were observed in this region for quite long periods of time at the beginning of experimental runs before they broke up into minute particles and became indistinguishable. It was therefore assumed that, the slow motion of kerosene droplets was an indication of the existence of dead volumes in the region. This condition resulted in low turbulence levels hence, the lower mass transfer rates that were observed.

The average change in mass transfer coefficients was 37.7% in the cone region. The reductions in mass transfer coefficients with the inclusion of the slag phase were about 38%, 39% and 36% for the gas flow rates 0.010 m^3/s, 0.015 m^3/s and 0.023 m^3/s respectively. A greater reduction in the mass transfer coefficient values near the cone region, than in the bottom region, was observed when the slag phase was included. This probably resulted from a combination of two factors. Firstly, the less exposure of the samples in the bottom region to the aggressive gas-liquid plume turbulent currencies, encountered near the cone region, meant that the samples experienced marginal changes originating from a reduced bath stirring power that resulted from slag inclusion. The major driving forces for samples' dissolution rates in the bottom region were eddies produced by the bath liquid bouncing off the bottom of the vessel. These eddies were most likely less affected by the reduction in specific stirring energy of the bath. Secondly, the reduction in turbulent currencies near the cone region as a result of the increased load impacted more on the mass transfer rates in this region. In the near cone region, mass transfer processes were mainly driven by purging gas stirring power related turbulence. The reduced influence of the step at the bottom of the vessel compounded to effects of a reduced gas stirring power near the cone region. Consequently, the effect of a reduced specific energy input was extensive as only less effective forces were available to promote mass transfer.

Samples near the bath surface region recorded the highest mass transfer rates. As explained earlier, the increased turbulence resulting from a much wider plume region plus the splashing action of the bath liquid was responsible for the high mass transfer rates. A sudden pressure drop at the bath surface also added to the turbulence in this region. Ed-

dies produced in the liquid by the gas leaving the bath at high velocity were responsible for the increase in the eroding power of the bath liquid in the vicinity of the bath surface.

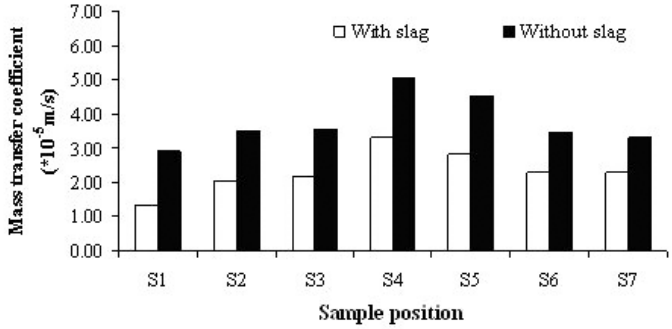

Figure 20: Comparison of mass transfer coefficient values at a gas flow rate of 0.015 m^3/s near the water bath surface region

The presentation in Figure 20 shows the effect of slag inclusion to mass transfer coefficients near the bath surface region. For all measurements taken, samples at Location S4 recorded maximum mass transfer coefficients. The plume effect at this location was marginal only in the bottom region, where the sample was not positioned inside the plume volume. The average change in mass transfer coefficients was 40% near the bath surface region. The reductions in the mass transfer coefficients with slag inclusion were about 33%, 39% and 48% for the gas flow rates 0.010 m^3/s, 0.015 m^3/s and 0.023 m^3/s respectively. Comparable average changes in mass transfer coefficient values near the cone region and water bath surface regions show that the inclusion of the slag phase had the same effect in the two regions. This was to be expected as mass transfer processes in both regions were mostly influenced by turbulence in the bath liquid resulting from bath purging.

CONCLUSIONS

Under conditions of a constant slag proportion in the bath, the mixing time was found to increase with bath height and decrease with gas flow rate. The mixing time data obtained was related to the specific energy dissipation rate. The established correlation, $T_{mix} = 4.39Q^{-0.73}W^{0.24}H^{1.12}$, was established to estimate the mixing time in the model vessel to an acceptable degree of accuracy. The correlation was upgraded to represent the industrial vessel for process control and designing purposes. Inclusion of the simulated slag phase resulted in the mixing time increasing by an average of about 16%. The mixing time was significantly prolonged at high levels of specific energy input to the bath and only marginally at very low specific energy levels.

The relationship showing derived mass transport coefficients (K) dependence on the gas injection rates (Q) was established as, $K \alpha Q^{0.08}$. The obtained relationship showed the little effect the increase in gas flow rate had on mass transfer, under the high gas stirring rates used in the CLU-converter operation. It was established that the bath liquid is in continuous circulation in an anti-clockwise motion with the leading edge above the gas purging nozzles. This motion provides for bulk mixing and mass transfer of the bath liquid in the vessel. However, turbulence characteristics inside the bath liquid were established to vary with location and gas injection rate. The bath surface region, the gas-liquid

plume region and the bath bottom region were established to exhibit higher mass transfer characteristics. The step at the bottom of the vessel increased turbulence by impeding the smooth bulk liquid flow. As a result, solid-liquid mass transfer characteristics of the bath increased in its locality.

REFERENCES

Nyoka, M., Akdogan, G., Eric, R. H. & Sutcliffe, N. (2003). *Metallurgical Transactions*. Vol. 34B, pp. 833-842. [1]

Nyoka, M. (2001). *Mixing & Mass Transfer in a Creusot Loire Uddeholm Converter*. MSc Dissertation, Witwatersrand University, Johannesburg, S. Africa.[2]

Lehner, T., Carlsson, G. & Hsiao, T. (1980). *Scaninject II, International Conference on Injection Metallurgy*. Vol. 1, pp. 22.1-22.34. [3]

Wright, J. K. (1989). *Metallurgical Transactions*. Vol. 20B, pp. 363-374. [4]

Akdogan, G. & Eric, R. H. (1999). *Metall. Trans*. Vol. 30B, pp. 231-239. [5]

Asai, S., Kawachi, M. & Muchi, I. (1983). *Scaninject III, Lulea*. Sweden, No. 12, pp. 1-29. [6]

Fruehan, R. J. & Martonik, L.J. (1978). *3rd International Iron & Steel congress Proceedings*. Chicago, IL, USA, April, pp. 229-238. [7]

Szekely, J., Lehner, T. & Chang, C. W. (1979). *Ironmaking & Steelmaking*, No. 6, pp. 285-293. [8]

Chaendera, A. & Eric, R. H. (2006). *Effects of a Simulated Slag Phase on Mixing & Mass Transfer Rates in a 0.2-Scale Creusot-Loire Uddeholm Converter Model*. TMS: Sohn International Symposium, Vol. 2, San Diego, California, U.S.A., pp. 263-270 . [9]

Akdogan, G. & Eric, R. H. (1999). *Metall. Trans*. Vol. 30B, pp. 231-239. [10]

Krishna Murthy, G. G., Mehrotra, S. P. & Ghosh, A. (1988). *Metallurgical Transactions*. Vol. 19B, pp. 839-850. [11]

Mazumdar, D., Kajani, S. K. & Ghosh, A. (1991). *Steel Res*. 61, 8, pp. 339. [12]

Krishna Murthy, G. G., Mehrotra, S. P & Ghosh, A. (1988). *Metallurgical Transactions*. Vol. 19B, pp. 839-850 [13]

Castillejos, A.H. & Brimacombe, J.K. (1989). *Metallurgical Transactions*. Vol. 20B, pp. 595-601. [14]

Chou, J. M., Chuang, M. C., Yeh, M. H., Hwang, W. S., Liu, S. H., Tsai, S. T & Wang, H. S. (2003). *Iron and Steelmaking*. Vol. 30, No. 3, pp. 195-202. [15]